Penerbit Akademia Baru

Malaysian Journal on Composites Science and Manufacturing

Journal homepage:
https://www.akademiabaru.com/submit/index.php/mjcsm/
ISSN: 2716-6945

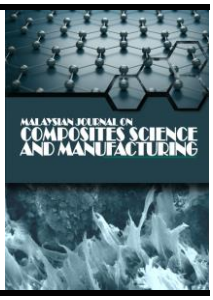

Mechanical Behaviors of the Single Crystal Two-Dimensional Silicon Carbide (SiC): A Molecular Dynamics Insight

Open Access

Tipu Sultan[1], Jahirul Islam[1,*], Md. Mehidi Hassan[1]

[1] Department of Materials Science and Engineering, Khulna University of Engineering & Technology, Khulna-9203, Bangladesh

ARTICLE INFO

Article history:
Received 30 August 2023
Received in revised form 13 November 2023
Accepted 16 November 2023
Available online 30 November 2023

ABSTRACT

This paper focuses on the two-dimensional silicon carbide (2D-SiC), which has an excellent opportunity to be used as an alternative to graphene in nanotechnologies such as in nanoelectronics, nanoelectromechanical systems (NEMS), nano-sensors, nano-energy harvesting devices, and nano-composites due to its unique structural, mechanical, electronic, and thermal properties. Their mechanical properties characterize the stability of the nanodevices. This study performs molecular dynamics (MD) simulation to examine the mechanical properties based on optimized Tersoff potential of the single crystal 2D-SiC at different temperatures, strain rates, point vacancies, and edge cracks. At room temperature (300 K), the obtained elastic modulus and fracture strength are 423 GPa and 68.89 GPa, respectively, along the armchair direction. As the temperature rises from 100 K to 800 K, the fracture stress falls by 21.96% and the fracture strain by 36.90%. An approximate linear reduction in fracture strength is noticed as the temperature rises from 100 K to 800 K. The elastic modulus also falls as the temperature rises but is not significant. Although the elastic modulus is unchanged, the fracture stress increases by 1.84% while the fracture strain increases by 5.84% for a change in strain rate from 0.0001 ps^{-1} to 0.005 ps^{-1}. The fracture stress and strain are significantly reduced, primarily due to the edge crack, as the concentration of point vacancy grows from 0.1% to 0.6% and the edge crack size increases from 0.5 nm to 1.5 nm. Moreover, anisotropic behavior is also evaluated at 300 K temperature and 0.001 ps^{-1} strain rate. These findings would offer a deep understanding of the fracture mechanics of 2D-SiC and also help to address the mechanical instability issue with SiC-based nanodevices.

Keywords:
Molecular Dynamics, Mechanical properties, 2D materials, Temperature effect, Strain rate effect

1. Introduction

Monolayer Silicon Carbide is a recently discovered honeycomb-like structure with a prevalent Si and C layer [1, 2]. For nanotechnology and nanoelectromechanical systems, Silicon Carbide is found

* *Corresponding author.*
E-mail address: jahirul@mse.kuet.ac.bd (Jahirul Islam)
E-mail of co-authors: sultan1727026@stud.kuet.ac.bd, mehidi27015@gmail.com

https://doi.org/10.37934/mjcsm.12.1.102113

to be highly promising for its superior and excellent electrical and mechanical properties [3]. Moreover, Silicon carbide nanosheets have been reported to be an extraordinarily favorable alternative to graphene owing to their outstanding thermal, mechanical, and structural properties [4]. However, the mechanical failure issue of the current nanoelectromechanical system (NEMS) is a significant challenge to its practical implementations [5]. Nevertheless, 2D-SiC has been implemented in many applications, such as lithium-ion batteries [6], semiconductor devices [7, 8], nanoelectronics [9], gas sensors [10], and energy harvesting systems [11].

Hundreds of 2D materials have been successfully produced, such as graphene, silicene, h-BN, SiC, GaN, ZnO, Phosphorene, and TMDs [12-16]. Graphene, the first 2D nanosheet of carbon atoms, demonstrates exceptional thermal, mechanical, and electrical capabilities [17]. In recent years, semi-2D or 2D silicon carbide layered systems have been successfully synthesized [18]. The molecular dynamics and finite element approach have been implemented to investigate the mechanical characteristics of SiC nanosheets and defect-induced states [19-21]. Recently, Wang *et al.* [22] and Makeev *et al.* [23] conducted a thorough investigation using molecular dynamics (MD) simulations to evaluate the nanomechanical behavior of pristine single crystalline SiC nanowires and good mechanical properties of pristine SiC have been reported.

Researchers found that material flaws significantly influence the mechanical and material properties of nanoscale materials due to their instability [24]. Ismail *et al.* [25] investigated the anisotropic mechanical behaviors of 2D SiC at various temperatures and vacancy defects using Vashishta potential. The interatomic potentials employed in molecular dynamics simulations exert a significant influence on the resulting physical properties [26]. Previous research has utilized a range of interatomic potential models, such as Tersoff, Stillinger-Weber (SW), MEAM, and Vashishta potential, to characterize the atomistic interactions of SiC nanomaterials [27]. The Tersoff potential has demonstrated its effectiveness by accurately replicating the phonon and thermal properties of these materials [28]. In addition, the elastic constants, cohesive energy, bulk modulus, and lattice constant of the SiC system obtained using the optimized Tersoff potential exhibit good agreement with density functional theory (DFT) calculations [29] and experimental results [30]. Fan *et al.* [31] obtained the elastic modulus of 433 GPa of SiC using the DFT method.

However, variations in the mechanical behavior of SiC monolayers subjected to various temperatures, strain rates, and defect concentrations using Tersoff potential have not yet been studied. This research investigated the mechanical behavior of pristine 2D-SiC nanosheets at various temperatures and strain rates using Tersoff potential. The changes in mechanical properties with induced defects, namely point vacancy and edge-crack with various concentrations and lengths, respectively, have also been explored in this study. At the start of the simulation, created monolayers were equilibrated for enough time steps to minimize the energy of the system and subsequent equilibration of all the thermodynamical parameters. The classical molecular dynamics simulation explored fracture strength and strain in the armchair orientations. Only the tensile properties in the X-X directions, precisely the armchair direction, were evaluated in this investigation.

2. Methodology

We used Classical molecular dynamics (MD) simulation software LAMMPS (Large-scale Atomic/Molecular Massively Parallel Simulator) [32] to analyze the mechanical behaviors of the single crystal SiC nanosheets at different temperatures and strain rates. Selecting an appropriate potential for a specific system is a prerequisite for generating satisfactory outcomes from MD modeling. The conventional Vashishta potential, an upgraded form of the Stillinger-Weber (SW) potential, has recently been created to evaluate the physical characteristics of the SiC system [33].

However, Tersoff and SW potentials are appropriate for silicon and carbon-based systems [28, 34]. The structural alteration of SiC under high pressure cannot be adequately described by SW potential. The Tersoff potential has effectively replicated the mechanical phenomenon of 2D-SiC and was in good agreement with previous DFT calculations [29]. So, in our work, we used the Tersoff potential generated by Tersoff [35] to clarify the atomic interactions among Si-Si, C-C, and Si-C particles. Moreover, employed Tersoff potential also includes terms with two- and three-body interactions, which is essential in precisely predicting the mechanical behavior of any system. Interatomic potential expression is written in Eq. 1 [35].

$$\phi_{ij}\left(r_{ij}\right) = \left[\phi_R(r_{ij}) - B_{ij}\,\phi_A(r_{ij})\right] \tag{1}$$

where, ϕ_R and ϕ_A represents repulsive and attractive pair interactions, B_{ij} denotes bond order terms in between atom $i\ and\ j$. The bond order term can be written as in Eq. 2.

$$B_{ij} = B(\psi_{ij}) \tag{2}$$

where, ψ_{ij} is a function that specifies the number of nearby atoms and the angles between them within a specific distance, describing how the atoms bond together [35].

$$V_{ij} = f_c(r_{ij})\left(A\,e^{-\lambda_1 r_{ij}} - B_{ij}e^{-\lambda_2 r_{ij}}\right) \tag{3}$$

$$B_{ij} = \left(1+\beta^n\zeta_{ij}^n\right)^{\frac{-1}{2n}}$$

$$\zeta_{ij} = \Sigma_{K\neq i,j}\, f_c(r_{ik})g(\theta_{ijk})e^{\lambda_2^3\left(r_{ij}-r_{ik}\right)^3} \tag{5}$$

$$g(\theta) = 1 + \frac{c^2}{d^2} + \frac{c^2}{(d^2+(h-\cos\theta)^2)} \tag{6}$$

$$f_c(r) = \begin{cases} 1, & r < R-D \\ \frac{1}{2} - \frac{1}{2}\sin\left[\frac{\pi}{2}(r-R)/D\right], & R-D < r < R+D \\ 0, & r > R+D \end{cases} \tag{7}$$

where in Equations 3 to 7, ζ_{ij} describes angular effects according to the number of potential pair bonds in the summation. $r_{ij} - r_{ik}$ the relative distance between two nearby atoms. λ denotes the bond strength and θ_{ijk} indicates the effective angle in between bonds ij and ik. $f_c(r_{ij})$ is a cut-off radius function.

Figure 1 depicts the armchair and zigzag chiral directions of the SiC nanosheet in its atomistic configuration and pictorial representation of point vacancy and edge crack. DFT obtained lattice parameters, and internal atomic coordinates were used to construct the crystal structure of the SiC. The VESTA platform created the 2D SiC nanosheet with a size of 151.38 nm^2 (17.4 nm long and 8.7 nm wide) and 6400 atoms. The 2D SiC structure was converted to a LAMMPS-compatible input file using the Atomsk program. For the uniaxial tensile loading, periodic boundary conditions were

applied in the X, Y, and Z directions. Vacuum space was produced along the Z-axis to stop atoms from interacting across the periodic boundary. The velocity Verlet algorithm was considered to calculate the interatomic forces between the atoms in the monolayer. The system's energy was minimized using the Conjugate Gradient (CG) algorithm before applying the tensile load. We used the canonical ensemble for 100 ps to stable the system's temperature to room temperature. In order to achieve pressure equilibrium, the system was subjected to an isothermal isobaric (NPT) ensemble for 40 ps at 1 bar before applying the constant strain rate of 10^9 s^{-1}. Although the employed strain rate is much greater than in real life, it is well suited for atomistic simulations to explore material failure processes with a manageable computational resource [36]. The applied stress tensor of the structure was calculated using the Eq. 8, following virial stress theorem [37]:

$$\sigma_{ij}^{\alpha} = \frac{1}{\Omega^{\alpha}}\left(\frac{1}{2}m^{\alpha}\mathrm{v}_i^{\alpha}\mathrm{v}_j^{\alpha} + \sum_{\beta=1}^{n}\mathrm{r}_{\alpha\beta}^{i}\mathrm{f}_{\alpha\beta}^{j}\right) \quad (8)$$

where $i, j =$ Cartesian coordinate system indices $\alpha, \beta =$ Atomic indices $m^{\alpha} =$ Mass of atoms $v^{\alpha} =$ velocity of the atoms $r_{\alpha\beta} =$ Atomic distance between α and β $f_{\alpha\beta} =$ Atomics force between α and β $\Omega^{\alpha} =$ Volume of atom α.

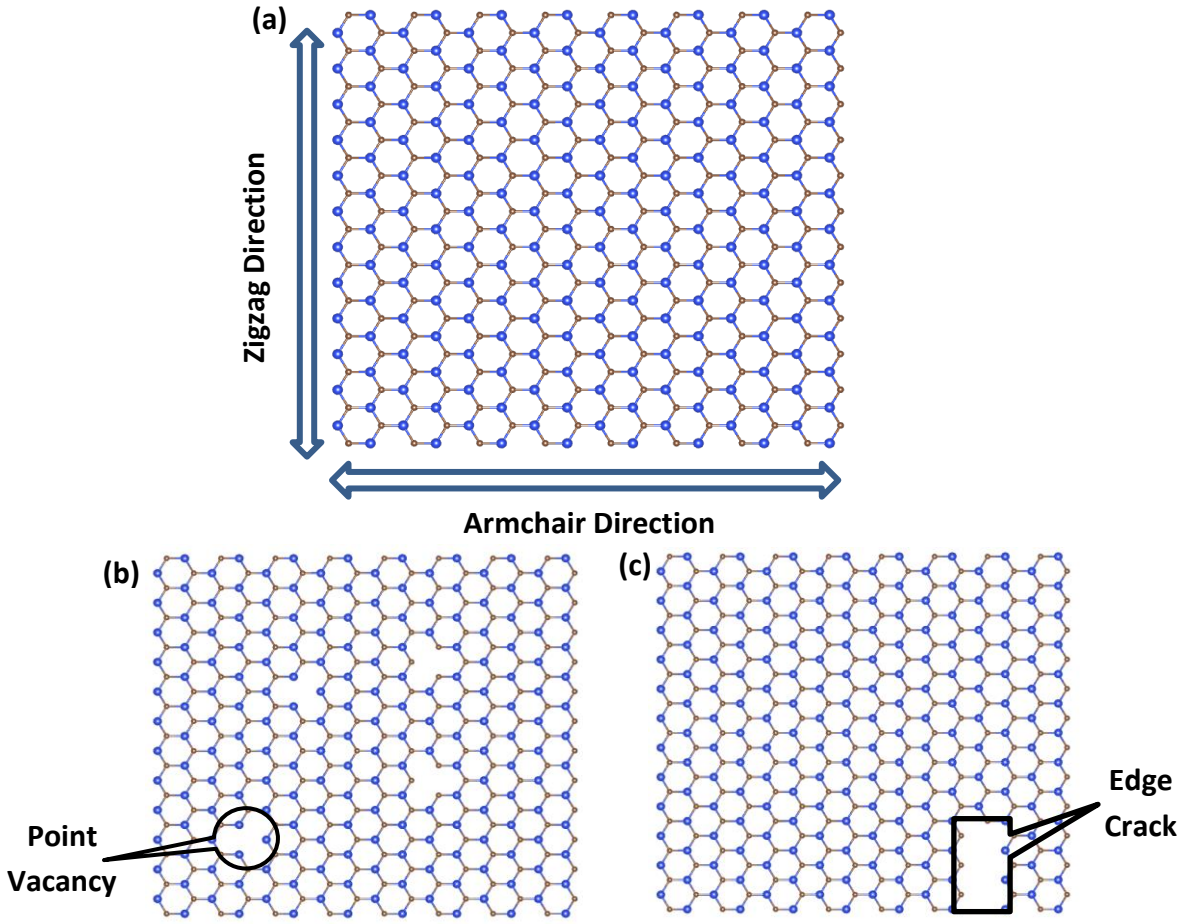

Fig. 1. (a) Loading components across the armchair and zigzag direction of monolayer-SiC; Pictorial representation of (b) point vacancy (c) edge crack in the monolayer

3. Results

3.1 Method Validation and Anisotropic Behavior

The elastic modulus was calculated only along the armchair direction as the stress-strain curve's initial portion aligns along the armchair and zigzag direction of the 2D-SiC monolayer. By applying the linear fit approach calculated elastic modulus is 423 GPa at the constant strain rate of 0.001 ps^{-1} and temperature of 300 K. The elastic modulus value obtained using the DFT method from the previously studied SiC monolayer is 433 GPa [31]. The deviations of the obtained values of elastic modulus are 2.3%. That means the simulated value obtained from this work is close to the previous study and thus justifies the employment of Tersoff interatomic potential.

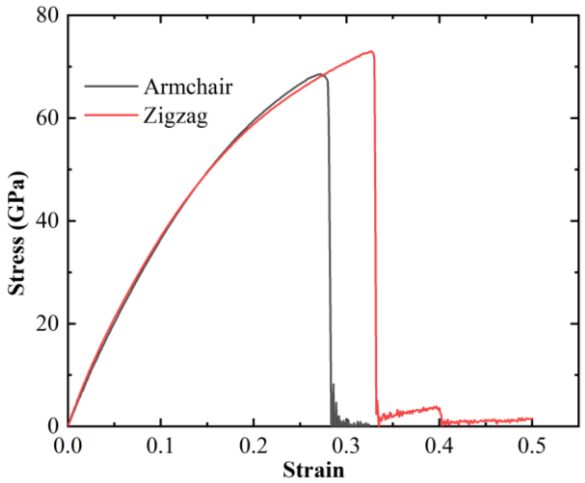

Fig. 2. Stress–strain relationships of SiC monolayer along the armchair and zigzag direction at 300 K temperature and 0.001 ps^{-1} strain rate

Figure 2 displays the effect of loading directions of the stress-strain response along the armchair and zigzag orientations at 300 K temperature and 0.001 ps^{-1} strain rate. Both armchair and zigzag-oriented 2D SiC exhibit a linear correlation between stress and strain almost up to the critical strength point, yield point, followed by a sharp drop corresponding to brittle fracture. At 300 K, the armchair-directed monolayer yields a maximum tensile strength of ~68.6GPa, whereas the zigzag orientation achieves a maximum of ~72.8GPa. Conversely, the critical fracture strains are 0.272 and 0.328 along armchair and zigzag orientations. This significant anisotropy in mechanical response along the two chiral orientations is typical behavior of 2D systems [25]. Each unit cell in the armchair orientation contains six stress-carrying bonds, four of which produced an angle of 60 degrees to the armchair loading direction and two parallel to the loading direction. In contrast, the zigzag orientation exhibits chirality at an angle of 30 degrees, with four stress-carrier bonds in each unit cell [25].

3.2 Effect of Temperature

2D nanomaterials must have good thermal stability at low and high temperatures to serve as high-quality nanodevices. Evaluation of the temperature-dependent mechanical behavior is therefore crucial. We simulated the SiC nanosheet from 100 K to 800 K to investigate the effect of temperature on mechanical characteristics under applied uniaxial tensile loading at a constant strain rate of 0.001 ps^{-1} along the armchair direction, as shown in Figure 3. When the temperature is 100 K, the 2D-SiC

sheet exhibits a fracture strength of around 75.46 GPa and a fracture strain of 0.336. However, when the temperature is raised to 800 K, the fracture strain and stress drop to 0.212 and 58.89 GPa, respectively. The fracture strain decreases by 36.90%, and the fracture stress decreases by 21.96% as the temperature increases from 100 K to 800 K. At normal temperature, the atomic oscillation of 2D-SiC is not as noticeable as at higher temperatures. However, when the temperature rises, the strength of the thermal vibration becomes more pronounced. As a result, the bond stress of the sheet decreases significantly, which harms the tensile properties of the 2D-SiC sheet. Tensile strength decreases with increasing temperature. As the temperature increases, the structure becomes less rigid due to the atom's thermal vibration. As a result, the chemical bond between Si and C becomes weaker. That is why, with increasing temperature, fracture strength and strain decreased.

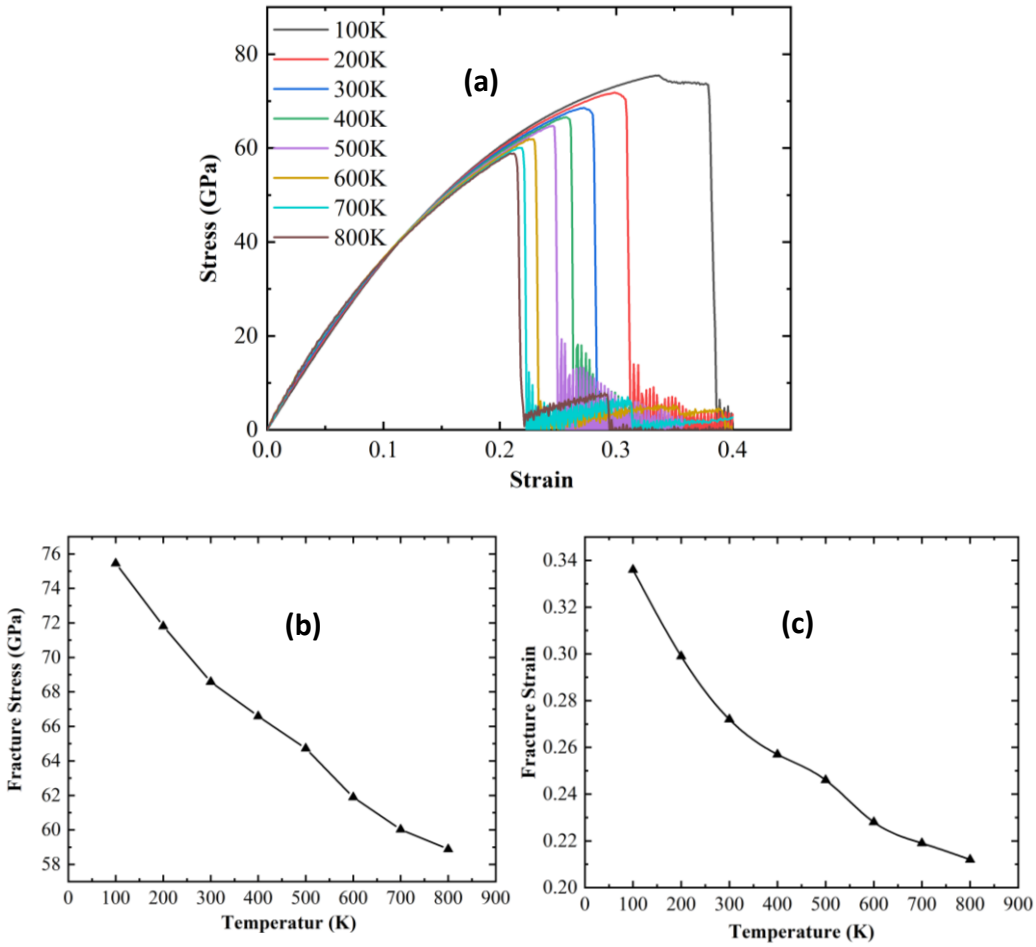

Fig. 3. (a) Stress-strain response of the SiC monolayer along the armchair direction at different temperatures and 0.001 ps^{-1} strain rate and Variations of (b) fracture stress, (c) fracture strain with temperature

3.3 Effect of Strain Rate

The applied loading variation can significantly impact the mechanical behavior of the nanosheets employed in practical applications. Notably, the fracture performances have significantly changed when the strain rate has changed. Here, we investigated strain rate effects from 0.0001 ps^{-1} to 0.005 ps^{-1} on the mechanical characteristics of 2D-SiC under uniaxial tensile strain at ambient temperature (300 K) as shown in Figure 4. Whereas the 2D-SiC sheet has a fracture strength of ~67.33

GPa and a failure strain of 0.257 at a strain rate of 0.0001 ps^{-1}, it increases to ~68.59 GPa and a fracture strain of 0.272 with a strain rate of 0.005 ps^{-1}. For the increase of the strain rate from 0.0001

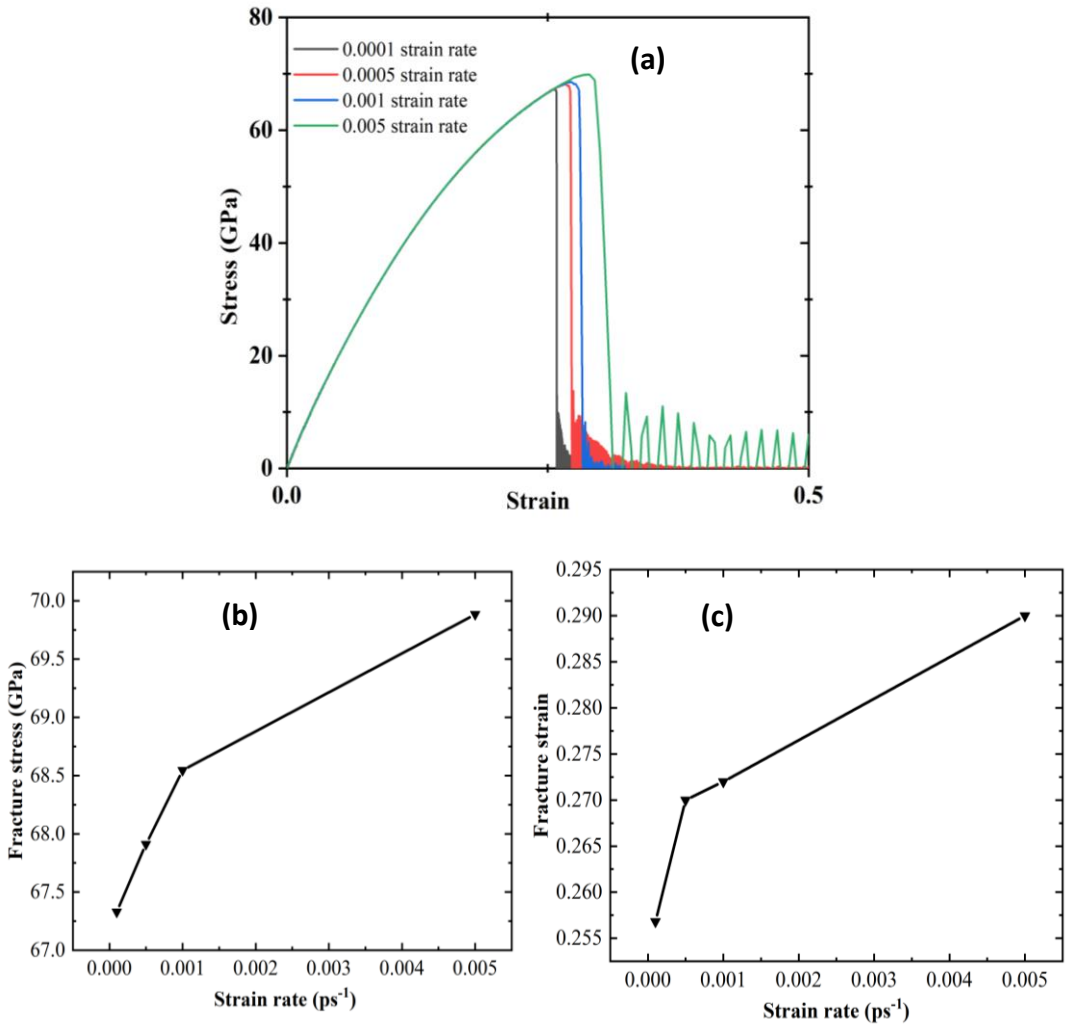

Fig. 4. Effect of strain rate on stress-strain behavior of SiC along (a) the armchair orientation and variations of (b) fracture stress, (c) fracture strain with strain rate at temperature 300 K

ps^{-1} to 0.005 ps^{-1}, the fracture stress rises by 1.84%, while the fracture strain rises by 5.84%. This characteristic makes sense since the material experiences uneven stress distribution when loaded at a high-speed strain rate. As a result, fracture strength and strain increase with increasing strain rate. However, the analysis demonstrates that strain rate has a relatively less impact on the mechanical behavior of the SiC monolayer.

3.4 Effect of Point Vacancy

This section looked into the mechanical behavior of 2D-SiC resulting from point vacancies. The stress-strain relationship of the point vacancy-defected sheet with vacancy concentrations varying from 0.1% to 0.6% at 300 K in the armchair position is shown in Figure 5(a). The fracture stress and strain along the armchair direction are predicted to be ~68.59 GPa and ~0.27 for a defect-free compound. Figures 5 (b) and (c) show that the fracture stress and strain decrease monotonically with increasing vacancy concentration. The 2D-SiC sheet has a fracture strength of ~66.99 GPa and a

fracture strain of 0.258 when the vacancy concentration is 0.1%. However, as the vacancy percentage is raised to 0.6, the fracture stress decreases to ~63.55 GPa, and the fracture strain decreases to 0.244. With a rise in vacancy concentration from 0.1% to 0.6%, the fracture stress drops by 5.14%, while the fracture strain is reduced by 5.43%.

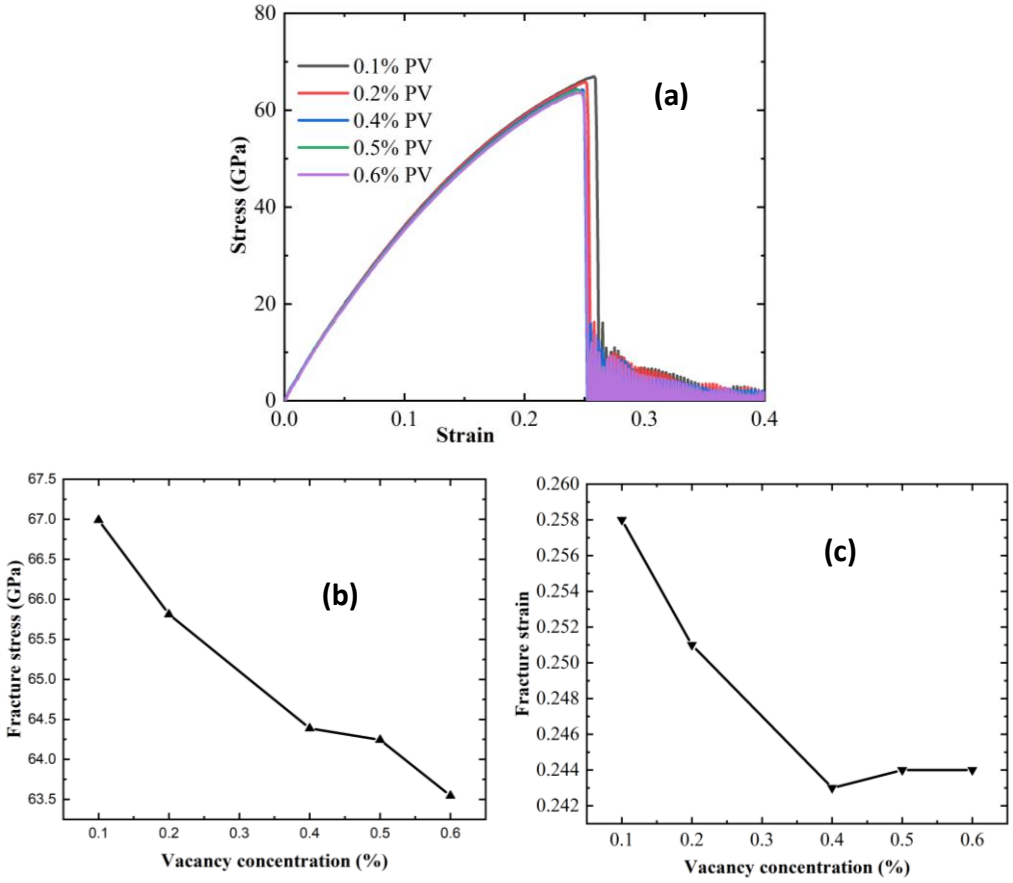

Fig. 5. Point vacancy induced (a) stress-strain behavior of SiC monolayer, and variations of (b) fracture stress, (c) fracture strain along the armchair direction

3.5 Effect of Edge Crack

Here, we modeled the uniaxial tensile characteristics of fractured SiC over a range of crack lengths to see how the material would perform. Pre-cracks are created by removing an atomic line in a zigzag pattern, and loads are applied perpendicular to the crack's length. Figure 6 shows how the fracture stress and strain change as the crack length increases. For the armchair loading circumstances, as shown in the picture, the material's tensile characteristics degrade with increasing crack length, and it fails at relatively low strain levels. This is expected as the stress concentration at the fracture tip increases with crack length [38].

The 2D-SiC sheet has a fracture stress of ~63.824 GPa and a strain of 0.236 when the crack length is 0.5 nm. However, when the crack length is increased to 1.5 nm, the fracture stress decreases to ~55.560 GPa, and the fracture strain decreases to 0.187. With a rise in crack length from 0.5 nm to 1.5 nm, the fracture stress is reduced by 12.95%, while the fracture strain is reduced by 20.76%. Similar detrimental features were also reported in previous studies on graphene, h-BN and MoS_2 [39, 40]. This shows wider cracks break bonds more rapidly by forming a plastic zone near the crack's tip.

Because of the extreme stress concentration at the fracture's tip, this plastic region experiences irreversible deformation, which paves the way for the crack to spread by breaking bonds [41]. As soon as a bond is broken, the structure will collapse catastrophically due to the brittle nature of silicon and carbon. Larger cracks may have weaker failure strengths because more atomic bonds are broken before the crack forms, throwing the structure's mechanical balance out of line. Even in the presence of significant cracks, the nonlinear behavior of the stress-strain curve of the SiC remains unchanged.

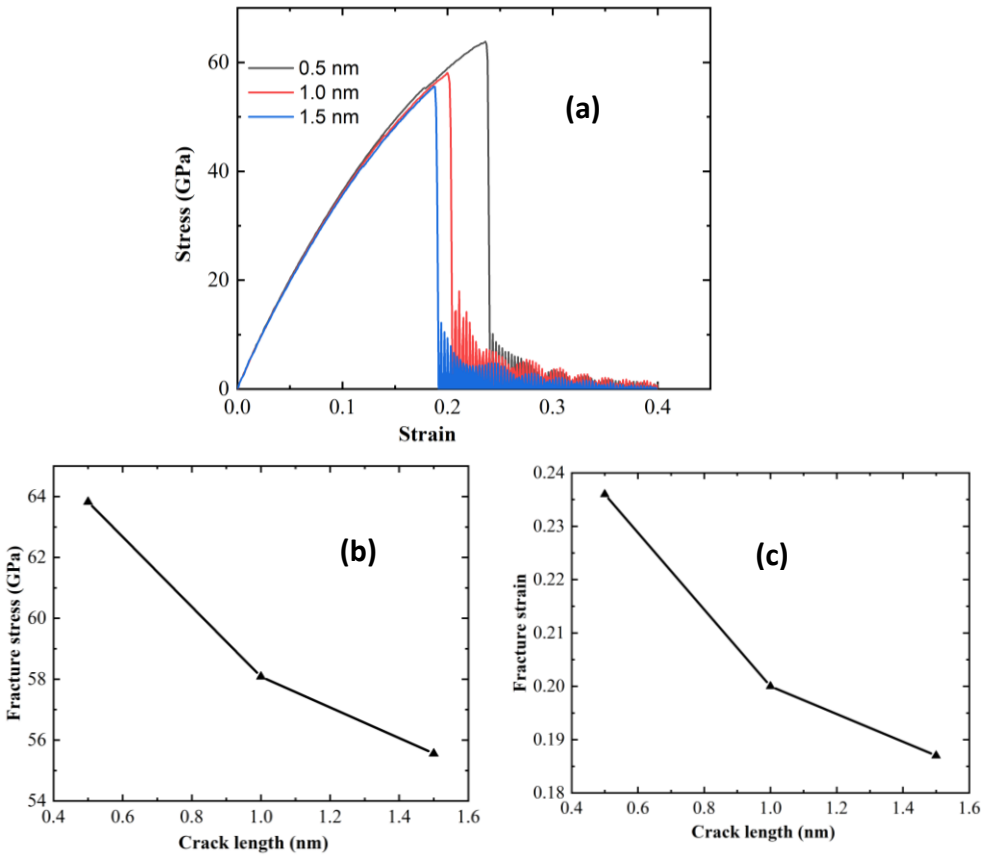

Fig. 6. Edge induced (a) stress-strain behavior of SiC monolayer, and variations of (b) fracture stress, (c) fracture strain along the armchair direction.

4. Conclusions

This extensive study examined how strain rate, temperature and defects affect the mechanical properties of 2D-SiC utilizing molecular dynamics simulation. The modified Tersoff potential was employed to gain a deeper understanding of these factors' effect on the mechanical characteristics of 2D-SiC. The outcome of the molecular dynamic simulation shows an excellent agreement of the mechanical properties of SiC with that of previously studied DFT data, as the values of elastic modulus were found to be 433 GPa, with only a 2.3% deviation. Increasing temperature causes a decrease in fracture strength and strain of the sample. Contrarily, strain rate shows the opposite effect as it has been observed to increase fracture strength and strain. The results from the defect-induced nanosheets of SiC show decreased mechanical behaviors with increasing point vacancy concentration and crack length. This study provides a clear insight into the mechanical performance of monolayer

SiC in various situations, which will be beneficial in developing nanoelectromechanical systems considering mechanical damage.

Acknowledgment
This work was performed at the Computational Materials Science Laboratory, Department of Materials Science and Engineering, Khulna University of Engineering & Technology, Khulna-9203, Bangladesh.

References

[1] Cahangirov, Seymur, Mehmet Topsakal, Ethem Aktürk, Hasan Şahin and Salim Ciraci, "Two-and One-Dimensional Honeycomb Structures of Silicon And Germanium," Physical Review Letters 102, no. 23 (2009): 236804. https://doi.org/10.1103/PhysRevLett.102.236804

[2] Shi, Zhiming, Zhuhua Zhang, Alex Kutana and Boris I. Yakobson, "Predicting Two-Dimensional Silicon Carbide Monolayers," ACS Nano 9, no. 10 (2015): 9802-9809. https://doi.org/10.1021/acsnano.5b02753

[3] Sun, Lian, Yafei Li, Zhenyu Li, Qunxiang Li, Zhen Zhou, Zhongfang Chen, Jinlong Yang and J.G. Hou, "Electronic Structures of SiC Nanoribbons," The Journal of Chemical Physics 129, no. 17 (2008): 174114. https://doi.org/10.1063/1.3006431

[4] Chabi, Sakineh and Kushal Kadel, "Two-Dimensional Silicon Carbide: Emerging Direct Band Gap Semiconductor," Nanomaterials 10, no. 11 (2020): 2226. https://doi.org/10.3390/nano10112226

[5] Xu, Man, Yarabahally R. Girish, Kadalipura P. Rakesh, Piye Wu, Honnayakanahalli M. Manukumar, Shayan M. Byrappa and Kullaiah Byrappa, "Recent Advances and Challenges in Silicon Carbide (SiC) Ceramic Nanoarchitectures and Their Applications," Materials Today Communications 28, (2021): 102533. https://doi.org/10.1016/j.mtcomm.2021.102533

[6] Olou'ou Guifo, Stéphane B., Jonathan E. Mueller, Diana van Duin, Mahdi K. Talkhoncheh, Adri CT van Duin, David Henriques, and Torsten Markus, "Development and Validation of a ReaxFF Reactive Force Field for Modeling Silicon–Carbon Composite Anode Materials in Lithium-Ion Batteries," The Journal of Physical Chemistry C 127, no. 6 (2023): 2818-2834. https://doi.org/10.1021/acs.jpcc.2c07773

[7] Cittanti, Davide, Enrico Vico and Lustin Radu Bojoi, "New FOM-based Performance Evaluation Of 600/650 V Sic and Gan Semiconductors for Next-Generation EV Drives," IEEE Access 10, (2022): 51693-51707. https://doi.org/10.1109/ACCESS.2022.3174777

[8] Jacobs, Keijo, Stefanie Heinig, Daniel Johannesson, Staffan Norrga and Hans-Peter Nee, "Comparative Evaluation of Voltage Source Converters with Silicon Carbide Semiconductor Devices for High-Voltage Direct Current Transmission," IEEE Transactions on Power Electronics 36, no. 8 (2021): 8887-8906. https://doi.org/10.1109/TPEL.2021.3049320

[9] Ortiz-Roldan, Jose M., Francisco Montero-Chacón, Elena Garcia-Perez, Sofía Calero, A. Rabdel Ruiz-Salvador and Said Hamad, "Thermostructural Characterization of Silicon Carbide Nanocomposite Materials via Molecular Dynamics Simulations," Advanced Composite Materials 31, no. 5 (2022): 485-504. https://doi.org/10.1080/09243046.2021.2001988

[10] Mercan, Kadir and Ömer Civalek, "Critical Buckling Load of SiCNTs: A Molecular Dynamics Study on Gas Sensing," International Journal of Engineering and Applied Sciences 14, no. 1 (2023): 40-52. https://doi.org/10.24107/ijeas.1151308

[11] Faghihnasiri, Mahdi, Mahyar Rezvani, Mostafa Shabani and Amir Hossein Firouzian, "The Temperature Effect on Mechanical Properties of Silicon Carbide Sheet Based on Density Functional Treatment," Solid State Communications 227, (2016): 40-44. https://doi.org/10.1016/j.ssc.2015.11.014

[12] Xu, Mingsheng, Tao Liang, Minmin Shi and Hongzheng Chen, "Graphene-like Two-Dimensional Materials," Chemical Reviews 113, no. 5 (2013): 3766-3798. https://doi.org/10.1021/cr300263a

[13] Butler, Sheneve Z., Shawna M. Hollen, Linyou Cao, Yi Cui, Jay A. Gupta, Humberto R. Gutiérrez, Tony F. Heinz *et al.*, "Progress, Challenges, and Opportunities in Two-Dimensional Materials Beyond Graphene," ACS Nano 7, no. 4 (2013): 2898-2926. https://doi.org/10.1021/nn400280c

[14] Wang, Qing Hua, Kourosh Kalantar-Zadeh, Andras Kis, Jonathan N. Coleman and Michael S. Strano, "Electronics and Optoelectronics of Two-Dimensional Transition Metal Dichalcogenides," Nature Nanotechnology 7, no. 11 (2012): 699-712. https://doi.org/10.1038/nnano.2012.193

[15] Chhowalla, Manish, Hyeon Suk Shin, Goki Eda, Lain-Jong Li, Kian Ping Loh and Hua Zhang, "The Chemistry of Two-Dimensional Layered Transition Metal Dichalcogenide Nanosheets," Nature Chemistry 5, no. 4 (2013): 263-275. https://doi.org/10.1038/nchem.1589

[16] Cahangirov, Seymur, Mehmet Topsakal, Ethem Aktürk, Hasan Şahin, and Salim Ciraci. "Two-and One-Dimensional Honeycomb Structures of Silicon And Germanium," Physical Review Letters 102, no. 23 (2009): 236804. https://doi.org/10.1103/PhysRevLett.102.236804

[17] Novoselov, Kostya S., Andre K. Geim, Sergei V. Morozov, De-eng Jiang, Yanshui Zhang, Sergey V. Dubonos, Irina V. Grigorieva and Alexandr A. Firsov, "Electric Field Effect in Atomically Thin Carbon Films," Science 306, no. 5696 (2004): 666-669. https://doi.org/10.1126/science.1102896

[18] Sun, Kaidi, Tongtong Wang, Weibo Gong, Wenyang Lu, Xin He, Eric G. Eddings and Maohong Fan. "Synthesis and Potential Applications of Silicon Carbide Nanomaterials/ Nanocomposites," Ceramics International 48, no. 22 (2022): 32571-32587. https://doi.org/10.1016/j.ceramint.2022.07.204

[19] Lin, Shisheng, Shengjiao Zhang, Xiaoqiang Li, Wenli Xu, Xiaodong Pi, Xiaoyi Liu, Fengchao Wang, Hengan Wu and Hongsheng Chen, "Quasi-Two-Dimensional SiC And SiC2: Interaction of Silicon and Carbon at Atomic Thin Lattice Plane," The Journal of Physical Chemistry *C* 119, no. 34 (2015): 19772-19779. https://doi.org/10.1021/acs.jpcc.5b04113

[20] Nguyen, Danh-Truong and Minh-Quy Le, "Mechanical Properties of Various Two-Dimensional Silicon Carbide Sheets: An Atomistic Study," Superlattices and Microstructures 98 (2016): 102-115. https://doi.org/10.1016/j.spmi.2016.08.003

[21] Chowdhury, Emdadul Haque, Md Habibur Rahman and Sungwook Hong, "Tensile Strength and Fracture Mechanics of Two-Dimensional Nanocrystalline Silicon Carbide," Computational Materials Science 197 (2021): 110580. https://doi.org/10.1016/j.commatsci.2021.110580

[22] Wang, Zhiguo, Xiaotao Zu, Fei Gao and William J. Weber. "Atomistic Simulations of the Mechanical Properties of Silicon Carbide Nanowires," Physical Review *B* 77, no. 22 (2008): 224113. https://doi.org/10.1103/PhysRevB.77.224113

[23] Makeev, Maxim A., Deepak Srivastava and Madhu Menon, "Silicon Carbide Nanowires Under External Loads: An Atomistic Simulation Study," Physical Review *B* 74, no. 16 (2006): 165303. https://doi.org/10.1103/PhysRevB.74.165303

[24] Gowthaman, S., T. Jagadeesha and V. Dhinakaran, "A Study on the Point Defect Effects on the Monolithic Silicon Carbide Tensile Features: A Molecular Dynamics Study," Silicon 14, no. 14 (2022): 8427-8438. https://doi.org/10.1007/s12633-022-01654-2

[25] Islam, ASM Jannatul, Md Sherajul Islam, Naim Ferdous, Jeongwon Park, Ashraful G. Bhuiyan and Akihiro Hashimoto, "Anisotropic Mechanical Behavior of Two Dimensional Silicon Carbide: Effect of Temperature and Vacancy Defects," Materials Research Express 6, no. 12 (2019): 125073. https://doi.org/10.1088/2053-1591/ab5a96

[26] Islam, ASM Jannatul, Md Sherajul Islam, Naim Ferdous, Jeongwon Park and Akihiro Hashimoto, "Vacancy-Induced Thermal Transport in Two-Dimensional Silicon Carbide: A Reverse Non-Equilibrium Molecular Dynamics Study," Physical Chemistry Chemical Physics 22, no. 24 (2020): 13592-13602. https://doi.org/10.1039/D0CP00990C

[27] Yan, Zefan, Rongzheng Liu, Bing Liu, Youlin Shao and Malin Liu, "Molecular Dynamics Simulation Studies of Properties, Preparation, and Performance of Silicon Carbide Materials: A Review," Energies 16, no. 3 (2023): 1176. https://doi.org/10.3390/en16031176

[28] Erhart, Paul and Karsten Albe, "Analytical Potential for Atomistic Simulations of Silicon, Carbon, and Silicon Carbide," Physical Review *B* 71, no. 3 (2005): 035211. https://doi.org/10.1103/PhysRevB.71.035211

[29] Karch, Krystian, P. Pavone, W. Windl, O. Schütt and D. Strauch, "Ab Initio Calculation of Structural and Lattice-Dynamical Properties of Silicon Carbide," Physical Review *B* 50, no. 23 (1994): 17054. https://doi.org/10.1103/PhysRevB.50.17054
[30] Lambrecht, W. R. L., B. Segall, Michael Methfessel and M. Van Schilfgaarde, "Calculated Elastic Constants and Deformation Potentials of Cubic SiC," Physical Review *B* 44, no. 8 (1991): 3685. https://doi.org/10.1103/PhysRevB.44.3685
[31] Fan, Qingyang, Changchun Chai, Qun Wei and Yintang Yang, "The Mechanical and Electronic Properties of Carbon-Rich Silicon Carbide," Materials 9, no. 5 (2016): 333. https://doi.org/10.3390/ma9050333
[32] Thompson, Aidan P., H. Metin Aktulga, Richard Berger, Dan S. Bolintineanu, W. Michael Brown, Paul S. Crozier, Pieter J. in't Veld *et al.*, "LAMMPS-A Flexible Simulation Tool for Particle-Based Materials Modeling at the Atomic, Meso, and Continuum Scales," Computer Physics Communications 271 (2022): 108171. https://doi.org/10.1016/j.cpc.2021.108171
[33] Vashishta, Priya, Rajiv K. Kalia, Aiichiro Nakano and José Pedro Rino, "Interaction Potential For Silicon Carbide: A Molecular Dynamics Study of Elastic Constants and Vibrational Density of States for Crystalline and Amorphous Silicon Carbide," Journal of Applied Physics 101, no. 10 (2007): 103515. https://doi.org/10.1063/1.2724570
[34] Lindsay, L. and D. A. Broido, "Optimized Tersoff and Brenner Empirical Potential Parameters for Lattice Dynamics and Phonon Thermal Transport in Carbon Nanotubes and Graphene," Physical Review *B* 81, no. 20 (2010): 205441. https://doi.org/10.1103/PhysRevB.81.205441
[35] Tersoff, J.J.P.R.B., "Modeling Solid-State Chemistry: Interatomic Potentials for Multicomponent Systems," Physical Review *B* 39, no. 8 (1989): 5566. https://doi.org/10.1103/PhysRevB.39.5566
[36] Zhang, Ying-Yan, Qing-Xiang Pei, Yiu-Wing Mai and Yuan-Tong Gu, "Temperature and Strain-Rate Dependent Fracture Strength of Graphynes," Journal of Physics D: Applied Physics 47, no. 42 (2014): 425301. https://doi.org/10.1088/0022-3727/47/42/425301
[37] Tsai, D.H., "The Virial Theorem and Stress Calculation in Molecular Dynamics," The Journal of Chemical Physics 70, no. 3 (1979): 1375-1382. https://doi.org/10.1063/1.437577
[38] Lepikhin, A.M., E.M. Morozov, N.A. Makhutov, and V.V. Leschenko, "Assessment of Failure Probabilities and the Allowable Size of Defects in Structural Elements Using the Criteria of Fracture Mechanics," Industrial Laboratory. Diagnostics of Materials 88, no. 3 (2022): 41-50. https://doi.org/10.26896/1028-6861-2022-88-3-41-50
[39] Rakib, Tawfiqur, Satyajit Mojumder, Sourav Das, Sourav Saha and Mohammad Motalab, "Graphene and Its Elemental Analogue: A Molecular Dynamics View of Fracture Phenomenon," Physica B: Condensed Matter 515, (2017): 67-74. https://doi.org/10.1016/j.physb.2017.04.009
[40] Subad, Rafsan ASI, Tanmay Sarkar Akash, Pritom Bose and Md Mahbubul Islam, "Engineered Defects to Modulate Fracture Strength of Single Layer MOS2: An Atomistic Study," Physica B: Condensed Matter 592 (2020): 412219. https://doi.org/10.1016/j.physb.2020.412219
[41] Mojumder, Satyajit, Abdullah Al Amin and Md Mahbubul Islam, "Mechanical Properties of Stanene Under Uniaxial and Biaxial Loading: A Molecular Dynamics Study," Journal of Applied Physics 118, no. 12 (2015): 124305. https://doi.org/10.1063/1.4931572